ELSEVIER

Chemical Engineering Journal 133 (2007) 187–194

Chemical Engineering Journal

www.elsevier.com/locate/cej

Performance of ethanol-fuelled solid oxide fuel cells: Proton and oxygen ion conductors

W. Jamsak [a], S. Assabumrungrat [a,*], P.L. Douglas [b], N. Laosiripojana [c], R. Suwanwarangkul [d], S. Charojrochkul [e], E. Croiset [b]

[a] *Center of Excellence in Catalysis and Catalytic Reaction Engineering, Department of Chemical Engineering, Faculty of Engineering, Chulalongkorn University, Thailand*

[b] *Department of Chemical Engineering, University of Waterloo, Canada*

[c] *The Joint Graduate School of Energy and Environment, King Mongkut's University of Technology, Thonburi, Thailand*

[d] *Department of Chemical Engineering, Faculty of Engineering, King Mongkut's Institute of Technology, Ladkrabang, Thailand*

[e] *National Metal and Materials Technology Center (MTEC), Thailand*

Received 31 July 2006; received in revised form 8 February 2007; accepted 1 March 2007

Abstract

This paper investigates the performance of ethanol-fuelled solid oxide fuel cells (SOFCs) with two types of solid electrolytes, namely oxygen ion-conducting (SOFC-O^{2-}) and proton-conducting electrolytes (SOFC-H^+). Our previous work reported that the SOFC-H^+ shows superior theoretical performance over the SOFC-O^{2-} electrolyte. However, in this work when all resistances are taken into account, the actual performance of the SOFC-O^{2-} (Ni-YSZ|YSZ|YSZ-LSM) becomes significantly better than that of SOFC-H^+ (Pt|SCY|Pt). The maximum power density of the SOFC-O^{2-} is about 34 times higher than that of the SOFC-H^+ when operated at an inlet H_2O:EtOH ratio of 3, a fuel utilization factor of 80% and a temperature of 1200 K. Then the required values of the total resistance of the SOFC-H^+ to achieve the same power density as the SOFC-O^{2-} were determined. It was found that due to the superior theoretical performance of the SOFC-H^+, it is not necessary to reduce the SOFC-H^+ total resistance to the same values as the one for SOFC-O^{2-}. The study also indicates that reduction of only the electrolyte resistance is not sufficient to improve the SOFC-H^+ performance and, therefore, the other resistances including activation, electrodes and interconnect resistances need to be reduced simultaneously. Finally, the improvement of the electrolyte resistance by changing its resistivity and thickness is discussed.

Keywords: Solid oxide fuel cell; Oxygen conductor; Proton conductor; Performance; Losses

1. Introduction

Fuel cells are considered to be the most promising technology for chemical to electrical energy conversion. Solid oxide fuel cells (SOFC) have attracted considerable interest as they offer a wide range of potential applications, possibility for operation with an internal reformer and high system efficiency. Many fuels have been suggested for use in SOFCs; among these, ethanol is considered to be an attractive green fuel because it can be produced renewably from biomass, waste materials from agro-industries, forestry residue materials, or even organic fractions from municipal solid waste. Ethanol also offers other advantages related to natural availability and safety in storage and handling.

There are a number of published studies dealing with the use of ethanol for producing hydrogen for use in fuel cells [1–7]. However, only a few studies of ethanol utilization in SOFCs operation have been undertaken. The performance of SOFCs fuelled by products from different ethanol processes, such as ethanol steam reforming, ethanol dry reforming and ethanol partial oxidation with air were investigated. Ethanol steam reforming showed the highest maximum efficiency for high operating temperature [8]. The performance of external reforming SOFC (ER-SOFC) with different fuels, such as methane, methanol, ethanol and gasoline, were compared over a temperature range of 800–1200 K [9]. The maximum efficiency was obtained near the boundary of carbon formation for all fuels. The highest efficiency was obtained from methane (96%) followed by ethanol (94%) and then methanol (91%). By using an exergy-energy analysis, it was reported that the methane-fed SOFC provides higher efficiency than when ethanol is fed [10].

* Corresponding author. Tel.: +66 2 218 6868; fax: +66 2 218 6877.
E-mail address: Suttichai.A@chula.ac.th (S. Assabumrungrat).

1385-8947/$ – see front matter © 2007 Elsevier B.V. All rights reserved.
doi:10.1016/j.cej.2007.03.003

Nomenclature

E	electromotive force (V)
E_a	activation energy (kJ mol^{-1})
F	Faraday's constant (C mol^{-1})
i	current density (A cm^{-2})
I	current (A)
K	equilibrium constant of hydrogen oxidation reaction (kPa$^{-0.5}$)
n_i	number of moles of component i (mol)
p_i	partial pressure of component i (kPa)
P	power density (W cm^{-2})
r	resistance (Ω cm^2)
r_{act}	activation polarization area specific resistance (Ω cm^2)
r_e	electrolyte area specific resistance (Ω cm^2)
r_o	other area specific resistance (Ω cm^2)
r_{tot}	total area specific resistance (Ω cm^2)
R	gas constant (J mol^{-1} K^{-1})
T	temperature (K)
V	voltage (V)
x_i	mole fraction of component i

Greek letters

δ	thickness (cm)
ρ	resistivity (Ω cm)

Subscripts

a	anode
c	cathode

Noticeably, most SOFC studies have employed oxygen-ion conducting electrolytes although proton-conducting electrolytes are also possible for SOFC operation. There are several studies on the development of proton-conducting ceramic electrolytes for high temperature applications [11–14]; however, these studies mostly focus on the characterization of material properties, such as conductivities under various atmospheres. To date, there are very few studies using proton-conducting electrolyte in an SOFC operation [15,16]. The performance of SOFC with proton-conducting electrolytes (SOFC-H^+) in Yb-doped $SrCeO_3$ (SCY) electrolyte with platinum electrodes system (Pt|SCY|Pt) were investigated. The SOFC-H^+ was tested with various fuels (H_2 and CH_4) and atmospheres (dry and wet) at high temperatures (873–1273 K). It was shown that the SOFC-H^+ (dry-CH_4) system provided the highest performance [16].

Theoretical performance comparisons of SOFCs with different electrolytes revealed that the SOFC-H^+ provides higher efficiency than the SOFC with oxygen-ion conducting electrolytes (SOFC-O^{2-}) for a system fed with hydrogen and methane [17,18]. However, these studies were based on the same steam/methane feed ratio for the methane-fed case. It was demonstrated in our previous work [19–21] that the steam requirement for the SOFC-O^{2-} is lower than that for the SOFC-H^+ due to the presence of steam generated by the anodic electrochemical reaction. Therefore, the benefit from lower steam requirements in the SOFC-O^{2-} should be taken into account in the comparison between the two processes. When this benefit was considered, it was still observed that the SOFC-H^+ yielded higher EMF and efficiency than the SOFC-O^{2-} [22]. However, the calculations neglected the presence of actual losses encountered in a real SOFC operation. Therefore, this article aims at comparing the actual performance of SOFCs with different electrolytes. Although it is well known that current proton-conducting electrolytes have high resistivity and thus the performance of SOFC-H^+ should be inferior to SOFC-O^{2-}, it is still necessary to determine the status of the SOFC-H^+ technology compared to that of SOFC-O^{2-}. In our previous work, the theoretical performance of SOFC-H^+ and SOFC-O^{2-} was compared. Only the EMF and maximum theoretical efficiency were considered at that time and no losses were taken into consideration. In contrast, this study focuses on the actual performance of SOFC-H^+ and SOFC-O^{2-}. The losses in the SOFC cell (e.g. activation losses and ohmic losses) are now considered. The information from this theoretical study is also important in determining property targets (e.g. resistivity, electrolyte thickness and other resistance) for SOFC-H^+ in order to yield similar performance as the SOFC-O^{2-}.

2. Theory

The reaction system involving in the production of hydrogen via ethanol steam reforming reaction is represented by the following reactions [23]:

$$C_2H_5OH + H_2O \rightarrow 4H_2 + 2CO \quad (1)$$

$$CO + H_2O \rightarrow H_2 + CO_2 \quad (2)$$

$$CO + 3H_2 \rightarrow CH_4 + H_2O \quad (3)$$

Previous results [24,25] confirmed that a gas mixture in thermodynamic equilibrium contains only five components of noticeable concentration: carbon monoxide, carbon dioxide, hydrogen, steam, and methane.

The following three reactions are the most likely reactions leading to carbon formation:

$$2CO \rightarrow CO_2 + C \quad (4)$$

$$CH_4 \rightarrow 2H_2 + C \quad (5)$$

$$CO + H_2 \rightarrow H_2O + C \quad (6)$$

The Boudard reaction (Eq. (4)) has the largest Gibb's free energy; therefore, it was used to determine the possibility of carbon formation. The carbon activity (α_c) can be calculated from the following equation:

$$\alpha_c = \frac{K_c p_{CO}}{p_{CO_2}} \quad (7)$$

where K_c represents the equilibrium constant in Eq. (4) and p_i is the partial pressure of component i. The carbon formation can take place when $\alpha_c \geq 1$ [9,26]. In this study, conditions for SOFC operation under carbon formation were avoided.

Two types of solid electrolytes can be employed; namely, oxygen-conducting and proton-conducting electrolytes, which differ in the location were water is produced. For the oxygen-conducting electrolyte, water is produced in the anode chamber whereas it appears in the cathode side for the proton-conducting electrolyte.

2.1. Voltage calculations

2.1.1. Electromotive force

The electromotive force (EMF) for different electrolytes can be calculated as follows:

$$\text{SOFC-O}^{2-}: \quad E = \frac{RT}{4F} \ln \frac{p_{O_2,c}}{p_{O_2,a}} \tag{8}$$

$$\text{SOFC-H}^{+}: \quad E = \frac{RT}{2F} \ln \frac{p_{H_2,a}}{p_{H_2,c}} \tag{9}$$

where p_{O_2} and p_{H_2} are oxygen and hydrogen partial pressures, respectively, while the subscripts 'a' and 'c' represent anode and cathode, respectively. R is the universal gas constant, T the absolute temperature and F is the Faraday's constant.

In SOFC-O^{2-}, the partial pressure of oxygen in the cathode chamber is calculated directly from its mole fraction whereas the value in the anode chamber is calculated by assuming that the oxygen content is in equilibrium with hydrogen and water. Accordingly, the oxygen pressure in the anode chamber is determined from the following equation:

$$p_{O_2,a} = \left(\frac{p_{H_2O,a}}{K p_{H_2,a}} \right)^2 \tag{10}$$

where K is the equilibrium constant of the hydrogen oxidation reaction.

In contrast, for the SOFC-H^+, the partial pressure of hydrogen in the anode chamber is determined directly from its mole fraction while that at the cathode side is determined by assuming that the hydrogen content is in equilibrium with oxygen and water. Accordingly, the hydrogen pressure in the cathode chamber is calculated from the following equation:

$$p_{H_2,c} = \frac{p_{H_2O,c}}{K p_{O_2,c}^{1/2}} \tag{11}$$

Since the gas composition typically varies along the chamber, so does the local EMF. Accordingly, the average EMF ($\bar{E}$) is determined by numerical integration of the local EMF per unit cell length. It should be noted that the EMF also depends significantly on the inlet H_2O:EtOH ratio, operating temperature and fuel utilization. To simplify the calculations, it is assumed that gas compositions at the anode are at their equilibrium compositions along the cell length. For the calculation of the equilibrium composition in the SOFCs the reader can refer to our previous work [19–22]. However, it should be noted that a deviation from this equilibrium condition would result in lower EMF values as less hydrogen was generated in the anode chamber to compensate for the hydrogen consumed by the electrochemical reaction. Therefore, the results shown in this work represent the best performances for all SOFC cases.

In this paper, the electrochemical cells composed of Ni-YSZ|YSZ|YSZ-LSM and Pt|SCY|Pt are considered for the SOFC-O^{2-} and the SOFC-H^+, respectively. In this study, the state-of-the-art Ni-YSZ|YSZ|YSZ-LSM was chosen to represent SOFC-O^{2-}. Pt|SCY|Pt was chosen for SOFC-H^+ because the SCY electrolyte is known as one of the classical proton conducting materials with a high proton transport number [13]. Indeed it has high chemical stability and high proton conductivity at high temperatures.

2.1.2. Actual voltage

In practice, there is a deviation between EMF and the actual cell voltage (V) due to several losses (e.g. ohmic loss, activation loss, etc.). The actual cell voltage (V) is determined as follows:

$$V = E - i r_{tot} \tag{12}$$

$$r_{tot} = r_e + r_o \tag{13}$$

$$r_o = r_{act} + r_{ohm,electrode} + r_{ohm,interconnect} \tag{14}$$

where i is the current density (A cm^{-2}), r_{tot} the total resistance (Ω cm^2), r_e the electrolyte resistance (Ω cm^2) and r_o is the other resistance (Ω cm^2) including activation, electrodes and interconnect resistances. In this article, it is assumed that fuels and oxidants are well-diffused in/out of the electrodes. Therefore, the concentration losses can be ignored. This assumption is valid when the SOFC does not operate at too high current density.

- Activation loss:

  Activation loss is the loss caused by electrochemical reactions at the electrodes. In this study, Achenbach's correlation [26] is used for calculations of the SOFC-O^{2-}:

$$\text{cathode}: \quad r_{act,c} = \left[\frac{4F}{RT} k (x_{O_2,c})^m \exp\left(-\frac{E_{a,c}}{RT} \right) \right]^{-1} \tag{15}$$

$$\text{anode}: \quad r_{act,a} = \left[\frac{2F}{RT} k (x_{H_2,a})^m \exp\left(-\frac{E_{a,a}}{RT} \right) \right]^{-1} \tag{16}$$

  where $x_{O_2,c}$ and $x_{H_2,a}$ are mole fractions of oxygen in the cathode chamber and hydrogen in the anode chamber, respectively. The parameters used in Eqs. (15) and (16) are summarized in Table 1. It should be noted that these parameters are valid in the temperature range of 1173–1273 K [27].

- Ohmic loss:

  Ohmic losses are caused by the resistance of materials (i.e., electrodes, interconnect and current collectors) from the flow of electrons and by the resistance of electrolyte from the flow of ions passing through it. Ohmic resistances can be calculated by using the following equations:

$$r_{ohm,i} = \rho_i \delta_i \tag{17}$$

Table 1
Parameters used in Eqs. (15) and (16)

r_{act} (Ω cm^2)	k ($\times 10^{-5}$ A cm^{-2})	E_a (kJ mol^{-1})	m
$r_{act,c}$	14.9	160	0.25
$r_{act,a}$	0.213	110	0.25

Table 2
Parameters of SOFC cell components in Eqs. (17) and (18)

Materials	Parameters		Thickness (μm)
	α (Ω cm)	β (K)	
Anode (40% Ni/YSZ cermet)	2.98×10^{-5}	−1,392	150
Cathode (Sr-doped $LaMnO_3$:LSM)	8.11×10^{-5}	600	2000
Electrolyte (Y_2O_3 doped ZrO_2:YSZ)	2.94×10^{-5}	10,350	40
Interconnect (Mg doped $LaCrO_3$)	1.256×10^{-3}	4,690	100
Protonic electrolyte (Yb doped $SrCeO_3$:SCY)	7×10^{-5}	5.5×10^{-3}	1000

with

$$\rho_i = \alpha_i \, e^{(\beta_i/T)} \tag{18}$$

where subscript i represents the cell component (i.e., electrodes, electrolyte and interconnect), ρ the resistivity, δ_i the thickness of component i, and α and β are the constants specific to the materials. The parameters used in these calculations are adopted from Chan et al. [28] for the SOFC-O^{2-} and from Iwahara [13] and Salar et al. [16] for the SOFC-H^+ and are shown in Table 2.

As the SOFC-H^+ is not as developed as the SOFC-O^{2-}, the resistances of the components in the cell are not available in the open literature. Consequently, the other resistance is derived from the deviation of the total resistance and the electrolyte resistance. The values of the total resistance are obtained from the literature [13]. It should be noted that the SOFC-O^{2-} model was verified by comparing the calculated maximum power density and its corresponding current density with the results from Hernandez-Pacheco et al. [29]. Small deviations between those results were observed, i.e., the maximum power density from the calculation at the current density of 0.75 A cm^{-2} is 0.33 W cm^{-2} compared to 0.30 W cm^{-2} as reported in the literature [29].

2.2. SOFC electrical efficiency

When current is drawn from the SOFC, the power density, P, in W cm^{-2}, produced can be calculated by:

$$P = iV \tag{19}$$

The electrical efficiency is defined as the ratio of electrical work produced by SOFC to the chemical energy contained in the fuel fed to the SOFC system as shown in the following equation:

$$\eta = \frac{IV}{n_{\mathrm{EtOH}}(\mathrm{LHV}_{\mathrm{EtOH}})} \tag{20}$$

where I is the total current (A) determined by numerical integration of the local current density along the cell length, $\mathrm{LHV}_{\mathrm{EtOH}}$ the lower heating value of ethanol at the standard condition (1235 kJ/mol) and n_{EtOH} is the molar flow rate of ethanol fed to the system.

3. Results and discussion

Fig. 1 shows the main characteristics of SOFC performances at different fuel utilizations for both SOFC-O^{2-} and SOFC-H^+.

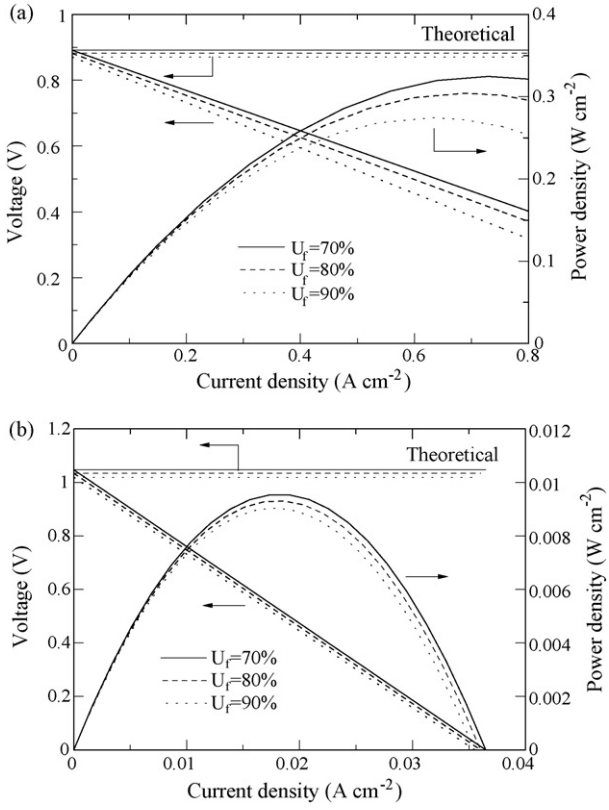

Fig. 1. Performance of SOFCs for various fuel utilizations: (a) SOFC-O^{2-} and (b) SOFC-H^+ (inlet H_2O:EtOH ratio = 3, T = 1200 K, P = 101.3 kPa, 400% excess air).

The calculations were based on a feed with an H_2O:EtOH ratio of 3 and temperature of 1200 K. The cell voltage decreases as the current density increases due to increasing losses. The power density initially increases with increasing the current density and drops at the higher values. For each value of fuel utilization, there is an optimum current density that maximizes the power density. The maximum power density decreases with increasing fuel utilization due to the effect of fuel depletion downstream. The observed values of the maximum power density of the SOFC-O^{2-} are within the range of the best value of 0.4 W cm^{-2} reported in the literature with an ethanol-fed system [30]. Fig. 1 also shows that the value of the current density for which the power density is maximum is essentially insensitive to the fuel utilization factor (at least in the range 70–90%) in the case of SOFC-H^+. The insensitivity of power density to fuel utilization in the case of SOFC-H^+ is due to the very large ohmic resis-

tance. The ohmic loss in the SOFC-H^+ electrolyte overshadows all other losses and since it is independent of the fuel utilization there is almost no difference in cell voltage for the different fuel utilizations, as seen in Fig. 1(a). As a consequence, the obtained maximum power density is insensitive to fuel utilization. For the SOFC-O^{2-}, the current density for which the power density is maximum decreases as the fuel utilization factor increases.

Performance comparisons between the two ethanol-fed SOFCs show that the SOFC-H^+ results in an EMF of around 1.01 V whereas it is approximately 0.89 V for the SOFC-O^{2-}. It is clear that the performance of SOFC-H^+ is theoretically superior to that of SOFC-O^{2-}, which is in good agreement with previous reports on SOFCs fed with H_2 and CH_4 [17,18] and ethanol [22]. The difference in the EMF between the SOFCs with different types of electrolytes is mainly due to the location of the steam generated by the electrochemical reaction, whether it is at the anode side for the SOFC-O^{2-} or at the cathode side for the SOFC-H^+. However, for an actual operation, losses strongly affect the performances of the SOFCs. It is clearly seen from Fig. 1 that the SOFC-H^+ does not perform as well as the SOFC-O^{2-}. The voltage in the SOFC-H^+ decreases significantly faster than that of the SOFC-O^{2-} as the current density increases, and the resulting maximum power density for the SOFC-H^+ is approximately 34 times lower than that of the SOFC-O^{2-}.

Another important indicator representing SOFC performance is the electrical efficiency defined in Eq. (20). The values of the electrical efficiencies at various current densities and fuel utilizations are illustrated in Fig. 2. When operating at a constant fuel utilization, the efficiency decreases with the increasing current density. The SOFC-H^+ can be operated over a much smaller range of current density than the SOFC-O^{2-} due to its higher losses. The maximum or theoretical efficiency is obtained when the current density approaches zero. At this condition, the SOFC-H^+ yields a higher efficiency than the SOFC-O^{2-} although it is not a practical operating condition as the power density is very low and, therefore, a large cell area would be required. When the fuel utilization increases, the efficiency increases although the opposite trend may be observed at high current densities, which yield low efficiency. It should be noted that the selection of suitable operating fuel utilization and current density is important as they influence the electrical efficiency and the power density, which are among the key parameters to evaluate SOFC performance.

The feed composition is another important parameter to be considered. From our previous work [22], it was reported that the SOFCs with different electrolytes required different inlet H_2O:fuel ratios to obtain their maximum EMFs. The effect of inlet H_2O:EtOH ratio on the voltage and power density is shown in Figs. 3 and 4, respectively. In the calculations, the fuel utilization was kept at 80% which is a typical operating condition used in the literature [27,29]. The inlet H_2O:EtOH ratio starts from its boundary of carbon formation which can be determined by following the procedure illustrated in our previous work [19–21]. It was found that the SOFC-O^{2-} yields the maximum voltage and power density at the boundary of carbon formation whereas those of the SOFC-H^+ are found at a ratio beyond the boundary of carbon formation. In order to compare the performance of

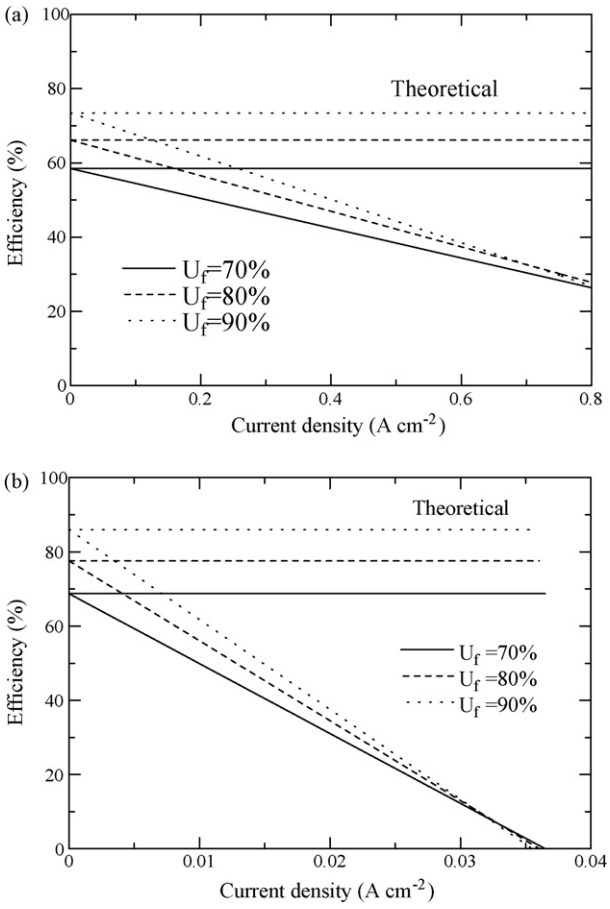

Fig. 2. Efficiency of SOFCs for various fuel utilizations: (a) SOFC-O^{2-} and (b) SOFC-H^+ (inlet H_2O:EtOH ratio = 3, T = 1200 K, P = 101.3 kPa, 400% excess air).

the SOFCs with different types of electrolytes, the best performance of each SOFC should be considered. The current density, H_2O:EtOH ratio and fuel utilization were varied to determine values which yield the highest power density for each type of SOFC.

Fig. 5 shows the maximum power density and the corresponding current density and inlet H_2O:EtOH ratio at different fuel utilizations. As expected, the maximum power density and the

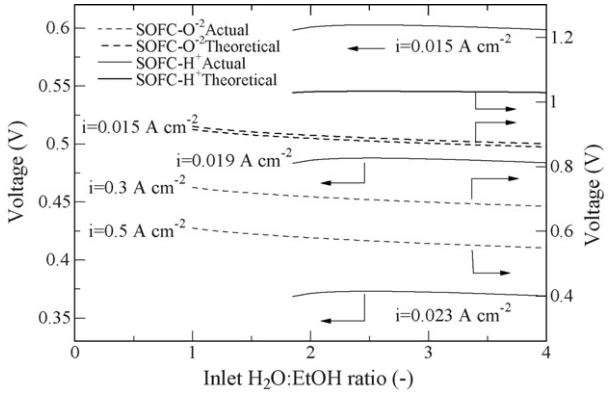

Fig. 3. Influence of inlet H_2O:EtOH ratio on voltage at various current densities (T = 1200 K, P = 101.3 kPa, U_f = 80%, 400% excess air).

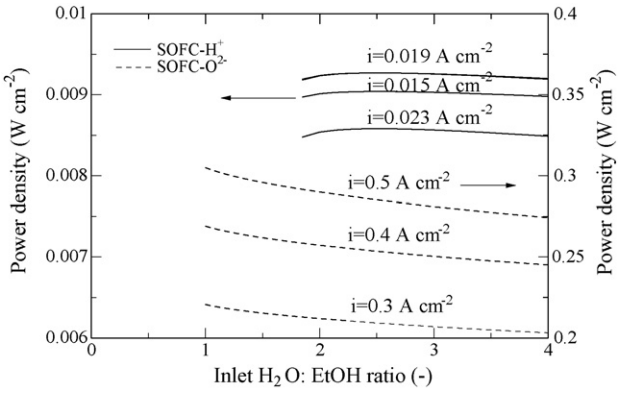

Fig. 4. Influence of inlet H_2O:EtOH ratio on power density at various current densities (T = 1200 K, P = 101.3 kPa, U_f = 80%, 400% excess air).

corresponding current density decrease with an increase in fuel utilization due to the effect of fuel depletion. Considering the corresponding values of the inlet H_2O:EtOH ratio, it can be noticed that for the SOFC-O^{2-} the values are independent of fuel utilization whereas it increases with increasing fuel utilization for the SOFC-H^+. The results can be explained by considering the influence of fuel utilization on the boundary of carbon formation. For the SOFC-O^{2-} case, the optimum H_2O:EtOH ratio is at the boundary of carbon formation. The fuel utilization does not affect the boundary of carbon formation because the critical condition for carbon formation occurs at the feed inlet in which the value of fuel utilization is zero. The possibility

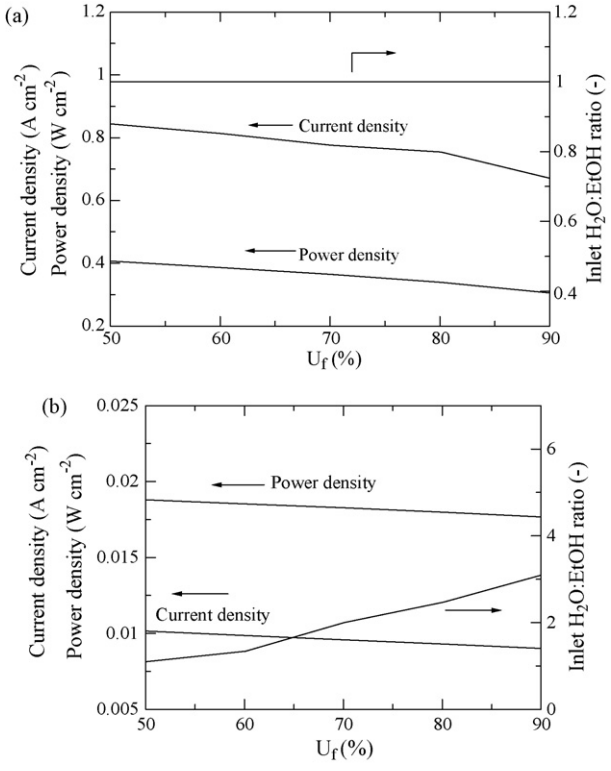

Fig. 5. Maximum power density of SOFC and their corresponding conditions (inlet H_2O:EtOH ratio and current density) at various fuel utilizations: (a) SOFC-O^{2-} and (b) SOFC-H^+ (T = 1200 K, P = 101.3 kPa, 400% excess air).

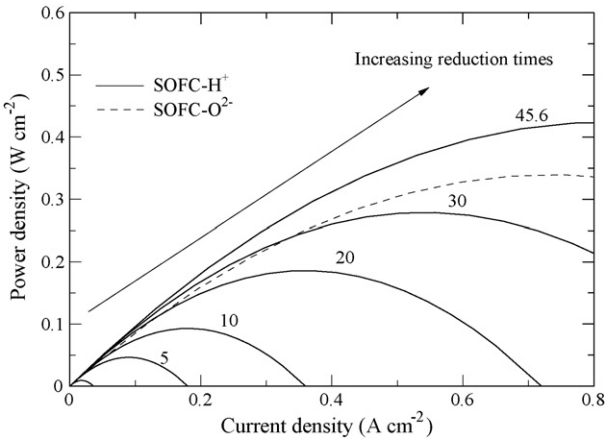

Fig. 6. Influences of total resistance on the performance of SOFC-H^+ compared with that of SOFC-O^{2-} (T = 1200 K, P = 101.3 kPa, 400% excess air).

for carbon formation becomes less severe when more hydrogen is consumed, i.e., higher fuel utilization, yielding water which helps suppress carbon formation. However, for the SOFC-H^+ case, at high fuel utilization, more hydrogen disappears without benefiting from the steam generated from the electrochemical reaction in the anode gas mixture, leading to higher possibility for carbon formation. Therefore, higher inlet H_2O:EtOH ratios are required to thermodynamically suppress carbon formation. From the results shown in Fig. 5, it is clear that the best performance of SOFC-H^+ is still lower than that of SOFC-O^{2-} for the entire range of fuel utilization, which confirms that the SOFC-H^+ does not show great promise, at least with the current extremely high resistance in SOFC-H^+.

To enhance the performance of SOFC-H^+, it is obvious that the resistance of the cell must be reduced due to the sudden drop in voltage. Fig. 6 depicts the influence of the total resistance of the SOFC-H^+ cell on the cell performances at 1200 K. It should be noted that the total resistance is termed as the summation of electrolyte resistance and the other resistances. In this section, the reduction time is defined as the ratio by which the total resistance is reduced compared to the current value. The dashed line represents the values of the SOFC-O^{2-}. Obviously, the total resistance is an important factor for improving the performance of SOFC-H^+. Higher power density can be obtained when decreasing the total resistance. It was found that when the total resistance of the SOFC-H^+ is reduced to 1/45.6 of the present value (28.7 $\Omega\,cm^2$), which would be equal to the total resistance of the current SOFC-O^{2-} (0.628 $\Omega\,cm^2$), the performance of the SOFC-H^+ is better than that of the SOFC-O^{2-}. It is clear that due to the superior theoretical performance of the SOFC-H^+, it is unnecessary to reduce the total resistance of the SOFC-H^+ to the level of that of the SOFC-O^{2-}. The total resistance in the SOFC-H^+, which yields an equivalent power density as the SOFC-O^{2-} is presented in Fig. 7 as function of temperature. It can be seen that a reduction by 1/30.7 (0.935 $\Omega\,cm^2$) is sufficient to offer the same power density as the SOFC-O^{2-} at 0.7 V and 1200 K. When increasing the operating temperature, the required resistance of SOFC-H^+ has to be further decreased due to a rapid decrease in the total resistance of SOFC-O^{2-}.

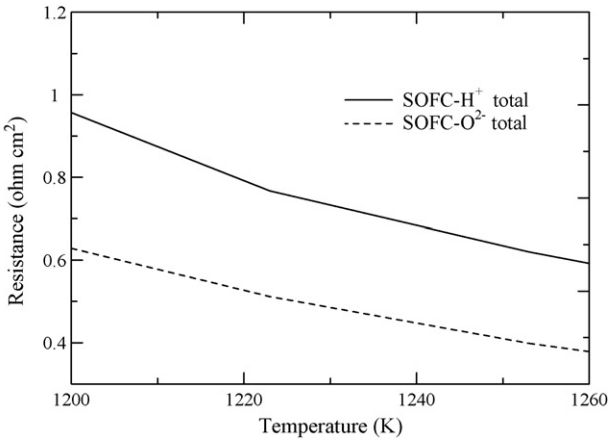

Fig. 7. Required total resistance of SOFC-H^+ with comparable SOFC-O^{2-} performance at various temperatures.

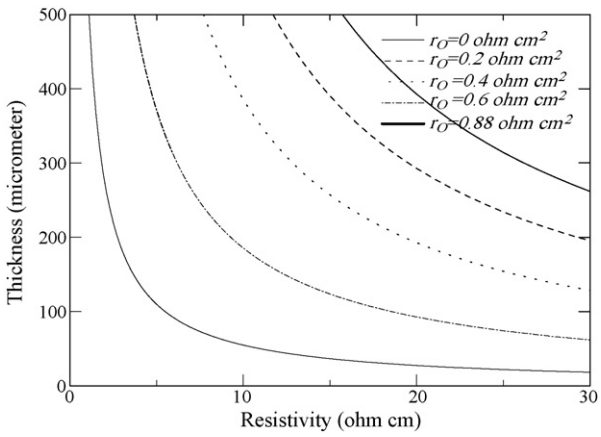

Fig. 8. Resistivity and thickness of proton-conducting electrolyte at various values of the other resistances, r_o (T = 1200 K, P = 101.3 kPa, 400% excess air).

Considering the Pt|SCY|Pt SOFC-H^+ cell in this study, the electrolyte, other and total resistances at 1200 K are 8.5, 20.2 and 28.7 $\Omega\,cm^2$, respectively. It is seen that the expected value of 0.935 $\Omega\,cm^2$ cannot be achieved by only reducing the electrolyte resistance. Both the electrolyte and the other resistances need to be improved simultaneously. At T = 1200 K, the electrolyte and the other resistances of the SOFC-H^+ are about 130 and 35 times, respectively, higher than those of the SOFC-O^{2-}. The high value of the other resistances of the SOFC-H^+ is possibly because platinum is not a good ionic conductor although it has high catalytic activity and high electronic conductivity [31]. In addition, since the cermet structure is not applied for the anode, the platinum is more likely to sinter rather than compacted to the electrolyte at high temperature [32]. These lead to low interfacial conductivity between the platinum electrodes and the electrolyte. From these comparisons, significant efforts are required to reduce both the electrolyte and the other resistances of the SOFC-H^+ cell.

Because the electrolyte resistance depends on its thickness and physical properties of material, it is possible to reduce the resistance by reducing the electrolyte thickness and/or using new materials with lower resistivity. Some materials with high proton conductivity have been reported, for example, $BaCe_{0.8}Y_{0.2}O_{3-\alpha}$ (BCY) and $BaCe_{0.9}Nd_{0.1}O_{3-\alpha}$ in which the resistivities at T = 1200 K are 12.5 and 28.6 Ω cm, respectively, compared to 85.0 Ω cm for the SCY used in this study [13]. Fig. 8 shows the required electrolyte thickness for different values of material resistivity of the electrolyte and the other resistance. It is clear that for a given value of the other resistance, the higher the material resistivity, the thinner the electrolyte is required. For the currently available high proton conducting material of SCY, when the electrolyte is reduced to a thickness as small as 150 μm which is in the range of an electrode-supported cell for 8YSZ [31], the other resistance should be reduced to 0.6 $\Omega\,cm^2$ which is approximately 1/33.7 that of the present value. To achieve the expected value of the other resistance, the electrical conductivities and activity of the cathode and anode must be significantly improved to replace the use of Pt. In addition, the interfacial resistivity between electrolyte/anode and electrolyte/cathode must be suppressed by a careful selection of material and suitable microstructure to enhance the triple-phase boundary. In addition, some other considerations such as mechanical strength, chemical compatibilities and thermal expansion compatibilities among the cell components need to be taken into account in the cell development. However, it is unfortunate that most of these data are currently not available. Therefore, considerable effort in the development of an SOFC-H^+ cell is necessary to eventually commercialize this type of fuel cell.

4. Conclusions

Although the theoretical EMF and electrical efficiency of the SOFC-H^+ are superior to those of the SOFC-O^{2-}, its actual voltage and power density are much lower than those of the SOFC-O^{2-} due to large resistance of the cell. It was calculated that in order to achieve an equivalent power density to the SOFC-O^{2-}, the total resistance of the SOFC-H^+ should be reduced to 0.935 $\Omega\,cm^2$, which is equal to 1/30.7 of the present value (28.7 $\Omega\,cm^2$), compared to the value of 0.628 $\Omega\,cm^2$ of the SOFC-O^{2-} at 1200 K. Due to the superior theoretical performance of the SOFC-H^+, it is unnecessary to reduce the total resistance of the SOFC-H^+ to the same value of the SOFC-O^{2-}. It was found that the reduction of the electrolyte resistance alone is not sufficient to reach the expected value of the total resistance. Both the electrolyte and the other resistances need to be improved simultaneously. The electrolyte resistance could be improved by reducing the electrolyte thickness and/or finding new materials with lower resistivity. When the electrolyte thickness of SCY, the currently available high proton conducting material, is reduced to 150 μm, in the range of an electrode supported cell for 8YSZ, the other resistance should be reduced to 0.6 $\Omega\,cm^2$ (1/33.7 of the present value). It is clear that the success of the SOFC-H^+ technology depends on the development of improved cell components.

Acknowledgements

The support from the Thailand Research Fund, Commission on High Education and National Metal and Materials Technology Center (MTEC) are gratefully acknowledged.

References

[1] S. Cavallaro, S. Freni, Ethanol steam reforming in a molten carbonate fuel cell. A preliminary kinetic investigation, Int. J. Hydrogen Energy 21 (1996) 465–469.

[2] G. Maggio, S. Freni, S. Cavallaro, Light alcohols/methane fuelled molten carbonate fuel cells: a comparative study, J. Power Sources 74 (1998) 17–23.

[3] T. Ioannides, S. Neophytides, Efficiency of a solid polymer fuel cell operating on ethanol, J. Power Sources 91 (2000) 150–156.

[4] T. Ioannides, Thermodynamic analysis of ethanol processors for fuel cell applications, J. Power Sources 92 (2001) 17–25.

[5] S. Cavallaro, N. Mondello, S. Freni, Hydrogen produced from ethanol for internal reforming molten carbonate fuel cell, J. Power Sources 102 (2001) 198–204.

[6] V. Klouz, V. Fierro, P. Denton, H. Katz, J.P. Lisse, S. Bouvot-Mauduit, C. Mirodatos, Ethanol reforming for hydrogen production in a hybrid electric vehicle: process optimisation, J. Power Sources 105 (2002) 26–34.

[7] N.A. Fatsikostas, D.I. Kondarides, X.E. Verykios, Production of hydrogen for fuel cells by reformation of biomass-derived ethanol, Catal. Today 75 (2002) 145–155.

[8] T. Tsiakaras, A. Demin, Thermodynamic analysis of a solid oxide fuel cell system fuelled by ethanol, J. Power Sources 102 (2001) 210–217.

[9] S.L. Douvartzides, F.A. Coutelieris, A.K. Demin, P.E. Tsiakaras, Fuel options for solid oxide fuel cell: a thermodynamic analysis, AIChE J. 49 (2003) 248–257.

[10] S. Douvartzides, F.A. Coutelieris, P.E. Tsiakaras, Exergy analysis of solid oxide fuel cell power plant fed by either ethanol or methane, J. Power Sources 131 (2004) 224–230.

[11] T. Shimada, C. Wen, N. Taniguchi, J. Otomo, H. Takahashi, The high temperature proton conductor $BaZr_{0.4}Ce_{0.4}In_{0.2}O_{3-\alpha}$, J. Power Sources 131 (2004) 289–292.

[12] T. Schober, F. Krug, W. Schilling, Criteria for the application of high temperature proton conductor in SOFCs, Solid State Ionics 97 (1997) 369–373.

[13] H. Iwahara, Proton conducting ceramics and their application, Solid State Ionics 86–88 (1996) 9–15.

[14] T. Schneller, T. Schober, Chemical solution deposition prepared dense proton conducting Y-doped $BaZrO_3$ thin films for SOFC and sensor devices, Solid State Ionics 164 (2003) 131–136.

[15] D. Browning, M. Weston, J.B. Lakeman, P. Jones, M. Cherry, J.T.S. Irvine, D.J.D. Corcoran, Proton conducting ceramics for use in intermediate temperature proton conducting fuel cells, J. New Mater. Electrochem. Syst. 5 (2002) 25–30.

[16] R. Salar, H. Taherparvar, I.S. Metcalfe, M. Sahibzada, Proceedings of the 2001 Joint International Meeting—The 200th Meeting of The Electrochemical Society Inc. and the 52nd Annual Meeting of the International Society of Electrochemistry, San Francisco, California, 2001.

[17] A. Demin, P. Tsiakaras, Thermodynamic analysis of a hydrogen fed solid oxide fuel cell based on a proton conductor, Int. J. Hydrogen Energy 26 (2001) 1103–1108.

[18] A.K. Demin, P.E. Tsiakaras, V.A. Sobyanin, S.Yu. Hramova, Thermodynamic analysis of a methane fed SOFC system based on a protonic conductor, Solid State Ionics 152–153 (2002) 555–560.

[19] S. Assabumrungrat, V. Pavarajarn, S. Charojrochkul, N. Laosiripojana, Thermodynamic analysis for solid oxide fuel cell with direct internal reforming fueled by ethanol, Chem. Eng. Sci. 59 (2004) 6015–6020.

[20] S. Assabumrungrat, N. Laosiripojana, V. Pavarajarn, W. Sangtongkitcharoen, A. Tangjitmatee, P. Praserthdam, Thermodynamic analysis of carbon formation in a solid oxide fuel cell with direct internal reformer fuelled by methanol, J. Power Sources 139 (2005) 55–60.

[21] W. Sangtongkitcharoen, S. Assabumrungrat, V. Pavarajarn, N. Laosiripojana, P. Praserthdam, Comparison of carbon formation boundary in different modes of solid oxide fuel cells fueled by methane, J. Power Sources 142 (2005) 75–80.

[22] W. Jamsak, S. Assabumrungrat, P.L. Douglas, N. Laosiripojana, S. Charojrochkul, Theoretical performance analysis of ethanol-fuelled solid oxide fuel cells with different electrolytes, Chem. Eng. J. 119 (2006) 11–18.

[23] S. Freni, G. Maggio, S. Cavallaro, Ethanol steam reforming in a molten carbonate fuel cell: a thermodynamic approach, J. Power Sources 62 (1996) 67–73.

[24] E.Y. Garcia, M.A. Laborde, Hydrogen production by the steam reforming of ethanol: thermodynamic analysis, Int. J. Hydrogen Energy 16 (1991) 307–312.

[25] K. Vasudeva, N. Mitra, P. Umasankar, S.C. Dhinggra, Steam reforming of ethanol for hydrogen production: thermodynamic analysis, Int. J. Hydrogen Energy 21 (1996) 13–18.

[26] E. Achenbach, Three-dimensional and time-dependent simulation of a planar solid oxide fuel cell stack, J. Power Sources 49 (1994) 333–348.

[27] E. Hernandez-Pacheco, D. Singh, P.N. Hutton, N. Patel, M.D. Mann, A macro-level model for determining the performance characteristics of solid oxide fuel cells, J. Power Sources 138 (2004) 174–186.

[28] S.H. Chan, C.F. Low, O.L. Ding, Energy and exergy analysis of simple solid-oxide fuel-cell power systems, J. Power Sources 103 (2002) 188–200.

[29] E. Hernandez-Pacheco, M.D. Mann, P.N. Hutton, D. Singh, K.E. Martin, A cell-level model for a solid oxide fuel cell operated with syngas from a gasification process, Int. J. Hydrogen Energy 30 (2005) 1221–1233.

[30] Fuel Cells Bulletin 8 (2005) 8.

[31] Handbook of Fuel Cells—Fundamentals, Technology and Applications, vols. 1–2, John Wiley & Sons Ltd., 2003.

[32] F.H. Garzon, R. Mukundan, R. Lujan, E.L. Brosha, Solid state ionic devices for combustion gas sensing, Solid State Ionics 175 (2004) 487–490.